



Potential Human Health Risks Due to Groundwater Fluoride Contamination: A Case Study Using Multi-techniques Approaches (GWQI, FPI, GIS, HHRA) in Bilate River Basin of Southern Main Ethiopian Rift, Ethiopia

Muhammed Haji¹ · Shankar Karuppannan¹ · Dajun Qin^{2,3} · Hassen Shube¹ · Nafyad Serre Kawo⁴

Received: 27 September 2020 / Accepted: 10 December 2020 / Published online: 3 January 2021
© The Author(s), under exclusive licence to Springer Science+Business Media, LLC part of Springer Nature 2021

Abstract

The main focus of the present research was to examine the appropriateness of groundwater resources for drinking purposes in the Bilate River Basin of Southern Main Ethiopian Rift, Ethiopia. The groundwater quality index (GWQI), fluoride pollution index (FPI), and human health risk were used to examine the human health risk factors associated with the intake of high fluoride groundwater. For this purpose, 29 groundwater samples were collected from the existing wells and were analyzed for various physicochemical parameters. The dominant cation was Na^+ , followed by Ca^{2+} , Mg^{2+} , and K^+ . The dominant anion was HCO_3^- , followed by Cl^- , SO_4^{2-} , and F^- . The Gibbs plot shows that rock-water interactions are the dominant factor controlling the groundwater chemistry. By using the GWQI, the quality of groundwater samples was 31% excellent, 21% good, 31% poor, and 17% very poor. The fluoride concentration in groundwater ranges from 0.2 to 5.60 mg/L (mean, 2.10 mg/L). 59% (i.e., 17 wells) of the groundwater samples were not suitable for drinking, because they surpassed the drinking water quality limit of 1.5 mg/L. The remaining 41% (i.e., 12 wells) of the samples were suitable for drinking. The FPI indicates that 51.72% of the wells were highly polluted by fluoride. The noncarcinogenic health risk varies from 0.75 to 8.44 for children (83%), 0.34–3.84 for women (62%), and 0.27–3.01 for men (52%), which indicates that children are at higher health risk than women and men due to the physiological condition and the rates of ingestion.

Groundwater is used as a tradable commodity in several parts of the world. In addition, it is widely used as an essential source for household, agricultural, industrial, and energy generation practices (Rufino et al. 2019; Wang et al. 2020; Wu et al. 2019). Groundwater is the significant source of water for human ingestion; therefore, variations in quality can have serious repercussions. In recent decades, prolonged

population explosions, economic growth, and global warming have adversely affected the quality of water (WWDR 2015; Singh and Kumar 2017; Yadav et al. 2019; Li 2016; Li et al. 2017, 2018). Water-quality studies usually cover the physicochemical and biological characteristics of water and its hydrochemical constituents, which are the most relevant variables in groundwater (Aravindan and Shankar 2011; Shankar et al. 2011b; Panneerselvam et al. 2020a). The physical and chemical properties of groundwater are largely dependent on various aquifer materials and hydrogeochemical processes as the water interacts with the lithological materials through which it flows (Prasad 1984; Todd and Mays 2005). Groundwater constituents also have been affected by land-based anthropogenic practices through infiltration, percolation, and recharging systems (Qin et al. 2013; Peng et al. 2018; Kavitha et al. 2019a, b; He and Wu 2019; He et al. 2019).

Geogenic and anthropogenic contamination of groundwater can cause harmful effects on human health as well as on socioeconomic growth (Mousazadeh et al. 2018; Kadam

✉ Shankar Karuppannan
geoshankar1984@gmail.com

¹ Department of Applied Geology, School of Applied Natural Science, Adama Science and Technology University, P.O. Box 1888, Adama, Ethiopia

² Key Laboratory of Shale Gas and Geoengineering, Institute of Geology and Geophysics, Chinese Academy of Sciences, Beijing 100029, China

³ Institute of Earth Science, Chinese Academy of Sciences, Beijing, China

⁴ School of Natural Resources, University of Nebraska-Lincoln, Lincoln, NE 68583-0996, USA

et al. 2019; Soujanya et al. 2020). The use of heavily polluted drinking water is the major cause of approximately 80% of waterborne diseases, especially in rural areas of developing countries, such as Ethiopia, India, and South Africa (WHO 2011; Saleem et al. 2016). Assessments of the quality of drinking water focus on the sustainability of clean water supplies, minimizing the threats to human health and maintaining ecosystem services for the aquatic environment (Shankar et al. 2011a; Wagh et al. 2019a, b; Balamurugan et al. 2020b). For 70% of the population in Ethiopia, groundwater serves the main source for community consumption, and it is observed that only 34% of the population has access to safe drinking water (IAEA 2013). It is worth assessing the quality of groundwater resources in Ethiopia as a significant step forward in developing water resource management.

Numerous researchers around the world have used various techniques, such as the groundwater quality index (GWQI), the fluoride contamination index (FPI), and health risk assessment (HRA), to understand groundwater mechanisms, quality, lithological-related hydrogeochemical processes, and human health threats due to high fluoride contamination of groundwater (Adimalla and Wu 2019; Li et al. 2019; Su et al. 2020a; Tian and Wu 2019). The GWQI is an effective tool used broadly to assess the groundwater quality for drinking purposes and to communicate the reliable information to the community (Saleem et al. 2016; Deepa and Venkateswaran 2018; Shankar and Kawo 2019; Mukate et al. 2019; Balamurugan et al. 2020a). Sajil Kumar (2017) recommended that the FPI be used to identify the high fluoride contamination of groundwater and its closely influenced factors (pH, Na/Ca ratio, and HCO_3^-), which facilitate the dissolution of the fluoride mineral in the environment at present. Several researchers have successfully utilized GIS for mapping the spatial distribution of different regions to assess the groundwater quality in their studies (Kawo and Shankar 2018; Amanuel 2018; Shankar and Kawo 2019; Getnet and Zelalem 2020). Health risk assessments are commonly used for the evaluation of human health risks due to various contaminants in drinking water (Arya et al. 2019; Adimalla 2019; Adimalla and Li 2019; Karunanidhi et al. 2020; Panneerselvam et al. 2020b; Shukla and Saxena 2020b). In recent decades, human health is at risk due to the consumption of high fluoride contaminated groundwater. Also in recent decades, researchers in several countries, such as China, Mexico, Brazil, Pakistan, India, and Sri Lanka, have documented their studies on elevated concentrations of fluoride in groundwater (He et al. 2020a; Vasquez et al. 2006; Rafique et al. 2008; Karunanidhi et al. 2020; Chandrajith et al. 2012).

However, the unplanned usage of groundwater resources for various purposes creates water scarcity and quality issues in different parts of the world (Varis 2014; Su et al. 2020b).

The Ethiopian Rift System occurs in complex hydrogeological settings (Haile and Abiye 2012), where considerable heterogeneity of aquifers (e.g., variable water levels) occurs over short distances (Furi et al. 2010; Kebede et al. 2010; Rango et al. 2012; Athick and Shankar 2019; Gebere et al. 2020). In addition, the use of groundwater in the Main Ethiopian Rift is hindered by its poor water quality due to the connection of geochemical anomalies with elevated fluoride concentrations, leading to concentrations that exceed the WHO drinking threshold of 1.5 mg/L (Rango et al. 2009, 2010; Haji et al. 2018).

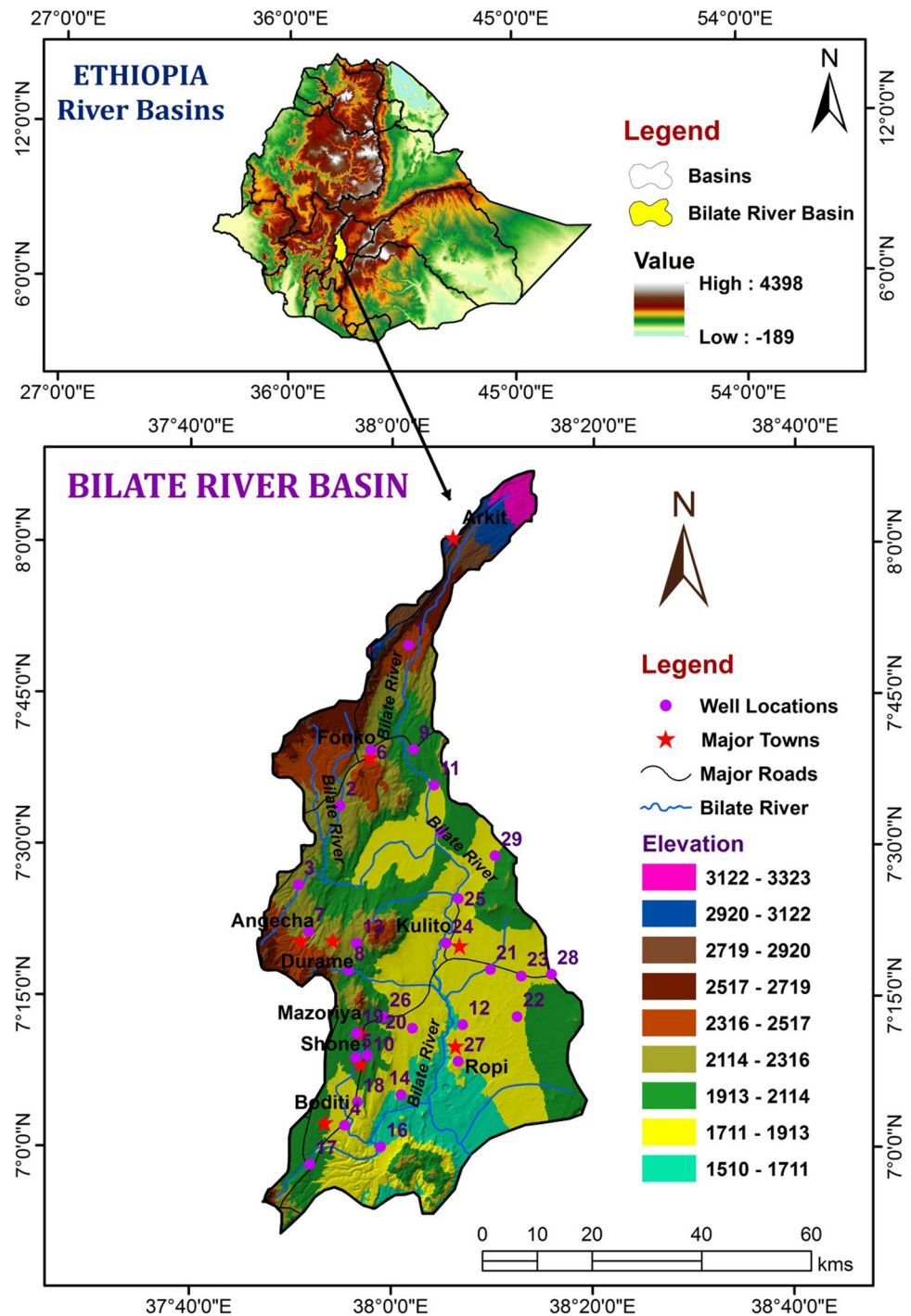
No detailed studies have been conducted in the Bilate River basin to assess the quality of groundwater and its impacts on human health. Hence, by focusing on the physicochemical characteristics of groundwater, the present study explores the Bilate River Basin with these objectives: (1) to characterize the geochemical parameters which influence groundwater quality; (2) to classify the quality of the groundwater using a Groundwater Quality Index; (3) to demarcate zones that are unsuitable as sources of drinking water because of elevated fluoride levels using the Fluoride Pollution Index and GIS; and (4) to assess human health risks due to elevated levels of fluoride in drinking water.

Materials and Methods

Study Area Description

The Bilate River Basin is situated in the Southern part of the Main Ethiopian Rift (MER). It is located in the Ethiopian rift valley lake basin bounded between $6^{\circ} 50' 0'' \text{N}$ – $8^{\circ} 07' 40'' \text{N}$ latitude and $37^{\circ} 40' 0'' \text{E}$ – $38^{\circ} 20' 0'' \text{E}$ longitude with altitudes ranging from 1510 to 3323 m above the mean sea level (Fig. 1). It is defined by the semi-arid climate on the rift floor and the humid climate on the eastern and western highlands. Topographically, it can be divided into three zones, such as the rift, escarpment, and physiographic highland zones. Annual rainfall in the rift varies dramatically from approximately 800 mm in the rift to 1500 mm in major parts of the highlands. The average annual precipitation over the basin is 1165 mm. The bimodal pattern of rainfall (March–May and July–October) is observed in the study area. The average monthly temperature of high altitude plateau (highlands) and the rift floor is 14°C and 22°C , respectively. The hydrology of the basin is largely controlled by the geology within the basin. In the uplands, the drainage systems flow in parallel with the geological structures. In the lowlands, a dendritic drainage pattern predominates.

Fig. 1 Location and altitudes of the study area

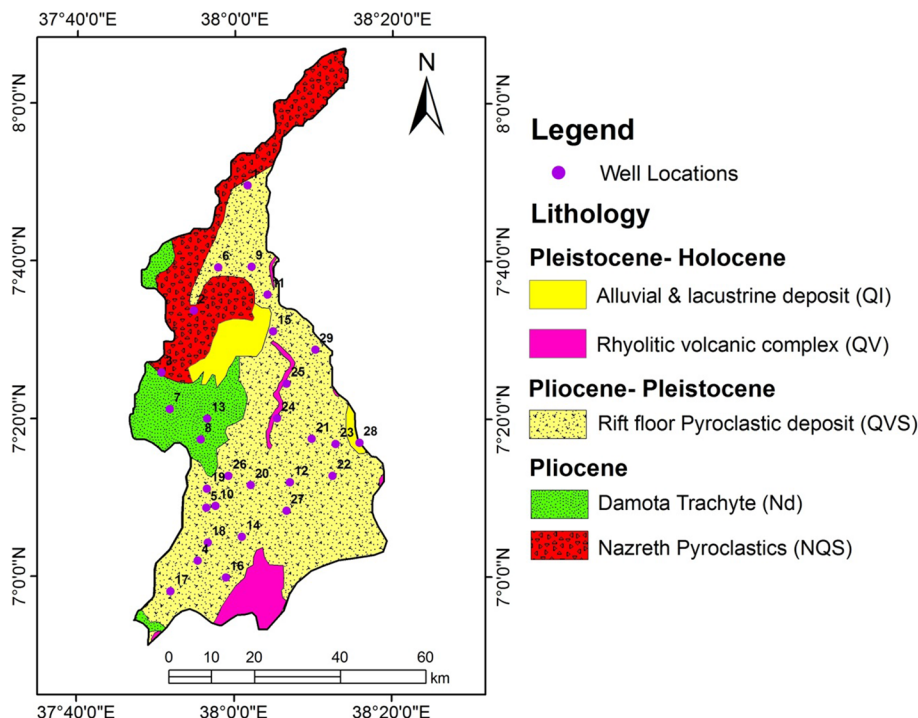


Geological and Hydrogeological Settings

Numerous volcanic activities which have happened in the main rift valley of Ethiopia have formed areas of thick volcanic rocks. The main types of rock identified in the region include trachytic, rhyolitic lava flows, basalt, unwedded tuff, ignimbrites, and pumice (Abbate et al. 2015; Hutchison et al. 2016). The Bilate River Basin in the northern highlands is dominated by volcanic quaternary rhyolites and trachytes,

whereas the Pleistocene and Holocene alluvial deposits of the Rift Valley are located in the lowlands of the basin, as shown in Fig. 2. The Bilate River Basin is mainly covered by the rift floor pyroclastic deposits (QVS), especially in the lowlands. The Pliocene units are covered by complex Pleistocene sequences with pyroclastic rocks and subordinate basaltic lava flows and lacustrine sediments. Volcanic sediments are formed on the rift floor of the Pleistocene, consisting of alluvial sands, pumiceous tuff, rhyolitic, and

Fig. 2 Geology map



basaltic fragments (Corti et al. 2013). Nazret pyroclastics (NQS) consists of the pervasive Pliocene peralkaline pantelleritic ignimbrites and the silicic volcanic complex of Damota volcano (Nd). Most of the rift floor is dominated by silicic pyroclastic deposits, consisting primarily of peralkaline rhyolitic ignimbrites, interlaced with basalts and tuffs, and filled with deposited and unwelded pumices (Tolera et al. 2020; Di Paola 1972). Alluvium sediments mainly occur along the lower reaches of the Bilate River and as patchy deposits along the rift's axial zone. In the study area, a lacustrine deposit varies in composition from clay to gravel. The lacustrine and alluvial deposit (QI) occurs in the small portion of the central and eastern part of the rift floor area. The sediments are mainly consisting of clay, sand, and silt deposits alternating with reworked pyroclastic deposits.

The aquifers of the basin are characterized by fractured volcanic rocks, sediments, and lacustrine deposits of the Tertiary and Quaternary age (Haji et al. 2018). The quaternary porous aquifer and the volcanic fissured aquifer are the typical hydro-stratigraphic units of the study area. Quaternary porous yield and Fissured volcanic aquifers vary from 3 to 14 L/s and from 2 to 5 L/s, respectively (Alemayehu 2006; Kebede 2013; Kebede et al. 2016). The depth to static water level ranges just below the land surface to ~290 m. The highland water-bearing areas are formed by the weathering volcanic rocks, inter-bedded with gravel and alluvium deposits. Alluvium-Lacustrine Sediments have moderate to high permeability and productivity, especially in the upper region of the Bilate River, where the subsurface well can yield up to 9 L/s, with fluctuating groundwater tables range from 1.5 to

50 m (Kebede 2013). In the basin, the western and northern parts are recharge zones and the central and southern parts are discharge zones. The groundwater depth increases from the highlands to the rift floor. The groundwater flows along the existing morphological slope from the western highlands to the eastern region along the rift. The average annual flow to the Bilate River is 108 m³/s (Hussen and Wagesho 2016). Annual groundwater recharge in the basin ranges from 0 to 385 mm, with an average of 114.2 mm (9–9.4% of annual precipitation). The majority (95%) of the annual groundwater recharge in the basin occurs during the rainy season (summer), while the remaining 5% occurs during the dry season (winter). The western areas in the Northern Highlands have a high annual groundwater recharge due to the permeable soils, high precipitation, and the deep-weathered and fractured volcanic rocks consistent with tectonic activity. These sources discharge to the rift floor as high discharge springs along the escarpment. In contrast, the central and southeastern areas have lower recharge due to low rainfall and impermeable soils (loam and silty loam soil).

Groundwater Sampling and Analytical Techniques

To appraise the groundwater quality of the Bilate River Basin, a total of 29 water samples were collected from both shallow and deep wells during the winter season (May 2016) and the locations of the wells are shown in Figs. 1 and 2. Standard pretreatment procedures (APHA 2012) were followed for sampling and analysis. Before sampling, the wells were pumped for 5–10 min to reduce the stored pipe water

in the well and to ensure sampling of the primary groundwater. High-density polythene bottles of 100-mL capacity were used as sample containers and the bottles were rinsed with 10% HNO₃ acid solution followed by distilled water for 2–3 times to avoid contamination. The latitude and longitude of the sample locations were noted by using a manual Global positioning system (GPS). Furthermore, the sample bottles were sealed, numbered, transported, and stored properly at 4 °C in the laboratory. The pH, electrical conductivity (EC), total dissolved solids (TDS), and temperature were analyzed in situ by using a Multi 3430 portable multiparameter water quality analyzer purchased from WTW (Weilheim, Germany), which was calibrated before use. Major anions (SO₄²⁻, Cl⁻, F⁻, and NO₃⁻) and cations (Ca²⁺, Mg²⁺, Na⁺, K⁺) were measured by ion chromatography using a Dionex DX-120 instrument with a conductivity detector purchased from Thermo Fisher (Waltham, MA). These major ions were analyzed by the Laboratory of Groundwater Dating, Institute of Geology and Geophysics, Chinese Academy of Sciences (IGG-CAS) in China. The limit of detection for fluoride was 0.01 mg/L, and limit of quantification was 0.03 mg/L. The working standards were measured after every five groundwater samples. The spiked recoveries ranged from 95.9 ± 7%, and the analytical precision of the measurements was 2–5% RSD. The details on the preparation and analysis of samples were previously described by Haji et al. (2018). Samples were analyzed in duplicate for quality assurance and quality control (QA/QC). To assess the accuracy of the analytical results, the Ionic Balance Error (IBE) was calculated according to Eq. 1 using data on all the major cations and anions measured in milliequivalents per litre (meq/L). IBE values are not supposed to surpass a limit of ± 5% (Hounslow 1995).

$$\text{IBE}(\%) = \frac{\sum \text{Cations} - \sum \text{Anions}}{\sum \text{Cations} + \sum \text{Anions}} \times 100 \quad (1)$$

Calculation of Groundwater Quality Index for Drinking Purpose

To determine the GWQI, the weights of the physicochemical parameters were assessed by referring to the significance of the overall quality of water for drinking purposes. GWQI computing was performed by using the following steps:

1. In the research, relative weighting (w_i) must be assigned to the groundwater parameters that have the potential to cause significant health effects (Kalaivanan et al. 2017; Kawo and Shankar 2018; Getnet and Zelalem 2020). F⁻ was assigned the highest value of w_i , followed in order, by TDS, NO₃⁻, HCO₃⁻, Ca²⁺, Na⁺, pH, EC, TH, Mg²⁺,

Cl⁻, and SO₄²⁻, and the lowest weight was assigned to K⁺, as shown in Table 1.

2. The relative weights (W_i) were obtained by the following Eq. 2:

$$W_i = \frac{w_i}{\sum_{i=1}^n W_i} \quad (2)$$

3. Quality ratio (Eq. 3),

$$q_i = \frac{C_i}{S_i} \times 100 \quad (3)$$

where q_i = quality rating scale for each parameter (i th), C_i = concentration of each parameter in water samples, and S_i = allowable limit for drinking set by WHO (2017).

4. Sub-index (Eq. 4),

$$\text{SI}_i = W_i \times q_i \quad (4)$$

5. Water quality index (Eq. 5),

$$\text{GWQI} = \sum \text{SI}_i \quad (5)$$

Based on the GWQI, the sources of groundwater were ranked as excellent, good, poor, very poor, or unsuitable for human consumption according to the range recommended by Sahu and Sikdar (2008) and Gaikwad et al. (2020), as shown in Table 2.

Table 1 Assigned and relative weight for GWQI computation with WHO standards (WHO 2017)

Physicochemical parameters	WHO (2017)	Weight (w_i)	Relative weight (W_i)
pH	6.5–8.5	4.0	0.087
EC (μS/cm)	1000	4.0	0.087
TDS (mg/L)	500	5.0	0.109
TH (mg/L)	100	3.0	0.065
Ca ²⁺ (mg/L)	75	4.0	0.087
Mg ²⁺ (mg/L)	50	3.0	0.065
Na ⁺ (mg/L)	200	4.0	0.087
K ⁺ (mg/L)	12	1.0	0.022
Cl ⁻ (mg/L)	250	3.0	0.065
HCO ₃ ²⁻ (mg/L)	120	4.0	0.087
SO ₄ ²⁻ (mg/L)	250	2.0	0.043
NO ₃ ⁻ (mg/L)	50	4.0	0.087
F ⁻ (mg/L)	1.5	5.0	0.109
		∑ w_i = 46.0	∑ W_i = 1.000

Table 2 Classification of computed GWQI ranges and types of water for human consumption

GWQI range	Type of water	GWQI rank
< 50	Excellent	1
50.01–100	Good	2
100.01–200	Poor	3
200.01–300	Very poor	4
> 300.01	Unsuitable	5

Table 3 Weight assigned to each of the water quality parameters included in the FPI calculation

Parameter	Concentration (mg/L)	Weight
F ⁻	< 0.6	1
	0.6–1.2	2
	1.2–1.5	3
	> 1.5	4
HCO ₃ ⁻	< 100	1
	100–200	2
	200–300	3
	> 300	4
Na ⁺ /Ca ²⁺	< 1	1
	1–2	2
	2–3	3
	> 3	4
pH	< 6.5	1
	6.5–7.5	2
	7.5–8.5	3
	> 8.5	4

Fluoride Pollution Index

The maximum acceptable limit for fluoride in drinking water is 1.5 mg/L (WHO 2011). The FPI is determined by summing the weighting of the groundwater concentrations of fluoride, bicarbonate, sodium/calcium ratio, and pH using Eq. 6. The values of the FPI range from 1 to 2 for low pollution, 2–3 for medium pollution, and 3–4 for high pollution (Sajil Kumar 2017).

$$FPI = \frac{W_f + W_{HCO_3} + W_{Na/Ca} + W_{pH}}{N} \quad (6)$$

where W_f is the weight assigned to fluoride, W_{HCO_3} is the weight assigned to bicarbonate, $W_{Na/Ca}$ is the weight assigned to the ratio between Na⁺ and Ca²⁺, and W_{pH} is the weight assigned to pH, as presented in Table 3. N is total number of groundwater parameters.

Health Risk Assessment

Based on exposure to fluoride through intake in drinking water and via dermal contact with contaminated water, the chronic daily intake (CDI) in drinking water and dermally absorbed dose (DAD) were calculated in units of mg/kg/day.

The noncarcinogenic risk via ingestion of drinking water was calculated using Eq. 7, as described by the US EPA (2001):

$$CDI = \frac{C \times IR \times ED \times EF}{BW \times AT} \quad (7)$$

where CDI indicates the chronic daily intake (mg/kg day). C signifies the concentration of fluoride in groundwater (mg/L). IR is the ingestion rate (L/day: 1.5 L/day for male and female, and 0.90 L/day for children). ED is the exposure duration (years: 30 for male and female, and 12 for children, respectively). EF is the exposure frequency (days/years: 365 days for children and male, female). BW is the average body weight (Kg: 70, 55 and 15 for male, female, and children respectively). AT is the average time (days: 10,950 for male and female, 4380 for children, respectively).

Dermal contact pathway is calculated by using the Eq. (8):

$$DAD = \frac{TC \times K_i \times EV \times ED \times EF \times SSA \times CF}{BW \times AT} \quad (8)$$

where DAD is the dermally absorbed dose (mg/kg day); TC is the contact duration (h/d) 0.4 for children male and female. K_i indicates the dermal adsorption parameters (cm/h: 0.001 cm/h). EV indicates the bathing frequency (times/day) 1 considered as time in a day). SSA is the skin surface area (cm²) 12,000 and 16,600 cm² for children and female, male respectively). CF indicates the conversion factors (0.001). ED is the exposure duration (years: 30 and 12 for male, female, and children, respectively). EF is the exposure frequency (days/years) 365 days for children, male, and female). BW indicates body weight (Kg: 70, 55 and 15 for male, female, and children, respectively). AT indicates the average time (days: 10,950 for male and female, 4380 children, respectively).

The for the fluoride health risks were estimated using the HQ_{oral} and HQ_{dermal} hazard quotients calculated by using Eqs. 9 and 10, respectively.

$$HQ_{oral} = \frac{CDI}{RfD} \quad (9)$$

$$HQ_{dermal} = \frac{DAD}{RfD} \quad (10)$$

RfD indicates the reference dosage of a particular contaminant. The RfD of fluoride is 0.04 mg/kg/day. The total

hazard index (THI), which signifies the noncarcinogenic risk is assessed by s hazard quotients ($HQ_{\text{oral}} + HQ_{\text{Dermal}}$) and are computed by Eq. (11):

$$THI_i = HQ_{\text{oral}} + HQ_{\text{dermal}} \quad (11)$$

Based on the estimated THI values, values < 1 indicate that there are no major risks for human health due to noncarcinogenic effects. However, THI values that surpass > 1 indicate health risks for the population (Li et al. 2016; USEPA 1989, 2001; He and Li 2020; He et al. 2020a, b).

Result and Discussion

Overall Groundwater Geochemistry

The statistical summary of the levels of the different physicochemical parameters in groundwater, as well as the limits of drinking water standards WHO (2017) are summarized in Table 4. The hydrogen ion (pH) values ranged from 5.6 to 8.17, with an average value of 7.16, indicating slightly acidic to nearly alkaline groundwater in the basin. High pH values indicate that there is groundwater circulation in the rift zone through faults and slow recharge of groundwater (Kawo and Shankar 2018). The electrical conductivity (EC) in groundwater ranged between 197 and 770 $\mu\text{S}/\text{cm}$, with an average value of 469.34 $\mu\text{S}/\text{cm}$ (Table 4). The TDS values in groundwater in the basin varied from 126.1 to 492.8 mg/L, with a mean value of 300.4 mg/L. Based on the EC and TDS values, all the groundwater samples were within the

allowable limits recommended by WHO (2017). Total hardness (TH) content in the samples varied from 24.19 to 208.96 mg/L, with an average value of 87.53 mg/L (Table 4). Approximately 24% of the groundwater samples had TH values that surpassed the desirable limit of 100 mg/L prescribed for drinking purposes (WHO 2017). The measured temperature in groundwater ranged from 22 to 41 °C (mean 26.3 °C). In fact, the temperature of groundwater reflects the environmental conditions by which the water flows in the subsurface. It has been observed that there is a progressive rise in temperature, TDS, EC, and pH values in groundwater from the highlands towards the rift floor, with the parameters influenced by thermal systems.

Na^+ followed by Ca^{2+} were the dominant cations in groundwater samples and HCO_3^- followed by Cl^- and SO_4^{2-} were the dominant anions in groundwater samples collected within the basin. Ca^{2+} concentrations ranged from 8.0 to 61.6 mg/L and Mg^{2+} concentrations ranged from 0.6 to 20.5 mg/L in groundwater within the basin, with average values of 22.7 mg/L and 7.5 mg/L, respectively. According to WHO (2017) drinking water guidelines, almost all water samples are suitable for drinking. This high concentration of Ca^{2+} and Mg^{2+} is due to the weathering of basic volcanic rocks (recent basalt) containing mafic silicate minerals, such as Olivine, Pyroxene, and amphibole, which are dominant in the highland aquifers (Ayenew 2008). Generally, the concentration decreases from the highland/escarpment waters toward the rift floor deep groundwater along the groundwater flow direction. Na^+ and K^+ were the dominant cations in groundwater samples collected from the rift floor. The Na^+ and K^+ values within the basin ranged from 7 to 106 mg/L

Table 4 Statistical summary of the different physicochemical parameters in groundwater

Ions	Minimum	Maximum	Mean	Std. dev	WHO (2017)		% of samples exceeding the permissible limits
					Most	Not	
					Desirable	Permissible	
pH	5.60	8.17	7.16	0.59	6.5 to 8.5	< 6.5 and > 8.5	10
EC ($\mu\text{S}/\text{cm}$)	197.00	770	469.34	170.79	< 1500	> 1500	0
T (°C)	22	41	26.3	4.47	–	–	–
TDS (mg/L)	126.08	492.80	300.38	109.30	< 500	> 1500	0
TH (mg/L)	24.19	208.96	87.53	42.97	< 100	> 500	24
Ca^{2+} (mg/L)	8	61.60	22.67	12.16	< 75	> 200	0
Mg^{2+} (mg/L)	0.60	20.50	7.51	4.26	< 50	> 150	0
Na^+ (mg/L)	7	106	43.48	20.81	< 200	> 200	0
K^+ (mg/L)	4.30	19	11.40	3.86	< 10	> 10	51
Cl^- (mg/L)	1.20	35.10	7.43	8.31	< 250	> 250	0
SO_4^{2-} (mg/L)	0	74.90	6.02	14.00	< 400	> 400	0
HCO_3^{2-} (mg/L)	26.80	622.60	338.10	175.31	< 300	> 600	59
NO_3^- (mg/L)	0.10	69.50	6.02	13.08	< 45	> 45	3
F^- (mg/L)	0.20	5.60	2.10	1.55	< 1.5	> 1.5	59

and 4.3 to 19 mg/L, respectively, with average values of 43.5 mg/L and 11.4 mg/L, respectively. The acceptable limit of Na^+ is 200 mg/L according to the WHO (2017), and all collected groundwater samples fell within this limit. The K^+ concentrations in groundwater from the study area were low when compared with other cations. The high relative Na^+ content of groundwater was mostly observed in deep aquifers, whereas high Ca^{2+} contents were observed in shallow aquifers. There was a trend of increasing values in groundwater from the highlands towards the rift floor. In the basin, the release of Na^+ into the groundwater is due to high rock-water interactions (basaltic to rhyolitic), with the weathering of acidic volcanic rocks occurring along the downstream portion of the basin.

HCO_3^- was the dominant anion in the river basin and the concentrations varied from 26.8 to 622.6 mg/L, with an average value of 338.1 mg/L. Of the groundwater samples in the basin, 59% exceeded the permissible limit of 300 mg/L (WHO 2017). The measured bicarbonate concentrations indicate an increasing trend from the highland towards the rift floor, which corresponds to the upsurge in sodium and potassium (Kawo and Shankar 2018). It is observed that in the Main Ethiopian rift, including the Bilate River basin, the reaction occurs between the dissolved CO_2 and the acidic volcanic rocks, resulted in a high concentration of HCO_3^- in groundwater (Demlie and Wohnlich 2006). The high partial pressure of CO_2 can be attributed to high bicarbonate, whereas ion-exchange contributed to the high Na content. The high temperature and high bicarbonate levels in the area are due to the high rate of magmatic outgassing of CO_2 that occurs through active fault zones (Mechal et al. 2017). The concentrations of Cl^- and SO_4^{2-} in the groundwater varied from 1.2 to 35.1 mg/L and below detection limits to 74.9 mg/L, with average values of 7.4 mg/L and 6.0 mg/L, respectively (Table 4). As per the WHO (2017) guidelines for Cl^- and SO_4^{2-} , all of the groundwater samples from the basin were under the acceptable limits of 250 mg/L and 400 mg/L, respectively. The high content of SO_4^{2-} observed in samples from the rift floor might be associated with volcanic emissions and lacustrine sediments. The concentrations of NO_3^- varied widely from below detection limits to 69.5 mg/L, with an average value of 6.02 mg/L (Table 4). A high concentration of NO_3^- was observed in only one sample collected from the northern part of the basin (i.e., sample number 1), which surpassed the permissible limit of 45 mg/L (WHO 2017). This might be due to pollution from agricultural activities such as the use of fertilizers, return flow of water during the process of irrigation and other anthropogenic activities (Aravindan et al. 2011; Shankar et al. 2011c). The concentrations of F^- in the basin groundwater varied from 0.2 to 5.6 mg/L, with an average value of fluoride of 2.10 mg/L (Table 4). The highest concentrations of F^- (i.e., 59% of samples) were observed in groundwater

samples collected from wells on the rift floor, and these values were greater than the 1.5 mg/L value set by the WHO (2017). In the main part of the Ethiopian rift floor, highly mineralized groundwater with longer residence times is observed in acidic volcanic rocks such as tuffs, fluvio/volcano lacustrine sediments, pyroclastic deposits, ignimbrite and rhyolite, and in high sodium-rich volcanic aquifers (Furi et al. 2011; Haji et al. 2018). Overall, the concentrations of cations and anions showed a slight trend of increasing levels in groundwater from the highland areas towards the rift floor (Table 4), which can be related to the evolution of groundwater parameters in transit towards the discharge area.

Hydrogeochemical Facies and Mechanisms Controlling the Groundwater Chemistry

The hydrogeochemical evolution of groundwater in the river basin is assessed by the concentration of major ions using the Piper diagram (Piper 1994). Several types of water have been identified, such as Ca-Mg-HCO_3 , Ca-Na-HCO_3 , Ca-Na-Mg-HCO_3 , Na-Ca-Mg-HCO_3 , Na-Ca-HCO_3 , Na-HCO_3 , Na-Mg-HCO_3 , Na-Mg-Ca-HCO_3 , Ca-HCO_3 , and Ca-Mg-Na-Cl-NO_3 . However, the dominant types of water are Ca-Mg-HCO_3 , Na-Ca-HCO_3 , and Na-HCO_3 . The Ca-Mg-HCO_3 is the dominant water type in the basic volcanic aquifers and Na-HCO_3 in the acidic volcanic aquifers. As shown in the piper diagram (Fig. 3), the groundwater in the basin shows a systematic hydrochemical evolution from the slightly mineralized and relatively young highland Ca-Mg-HCO_3 water type to the moderately mineralized rift escarpment Na-Ca-HCO_3 water type and finally to the highly mineralized and Na-HCO_3 water type along the groundwater flow path from the highland to the rift floor. Ca-Mg-HCO_3 type waters from the highland area are most likely the result of interactions with basaltic rock and alluvial deposits in the areas where the main composition of basalt is Ca^{2+} and Mg^{2+} . The Ca-Mg-HCO_3 and Ca-HCO_3 groups represent groundwater with the early stages of geochemical evolution (recent recharge) and rapid circulation of groundwater that have not undergone significant water-rock interactions due to fractured basalt, rhyolites, and ignimbrites (Ayenew 2008; Yitbarek et al. 2012; Furi et al. 2012). $\text{Na-Ca-HCO}_3/\text{Na-HCO}_3$ water type increases the electrical conductivity, the residence of times and water-rock interaction. In addition to that, the silicate hydrolysis with gaseous CO_2 results in the release of HCO_3^- to Ethiopian rift groundwater (Mechal et al. 2017).

In the present research, the Gibbs diagram (Gibbs 1970) is used to identify the hydrogeochemical processes required for groundwater geochemistry. In the basin, anion and cation Gibbs plots reveal that all the groundwater samples fall in the rock-water interaction field, as shown in Fig. 4. It indicates that the rock-water

Fig. 3 Piper trilinear plot showing the water types in the groundwater samples of the basin

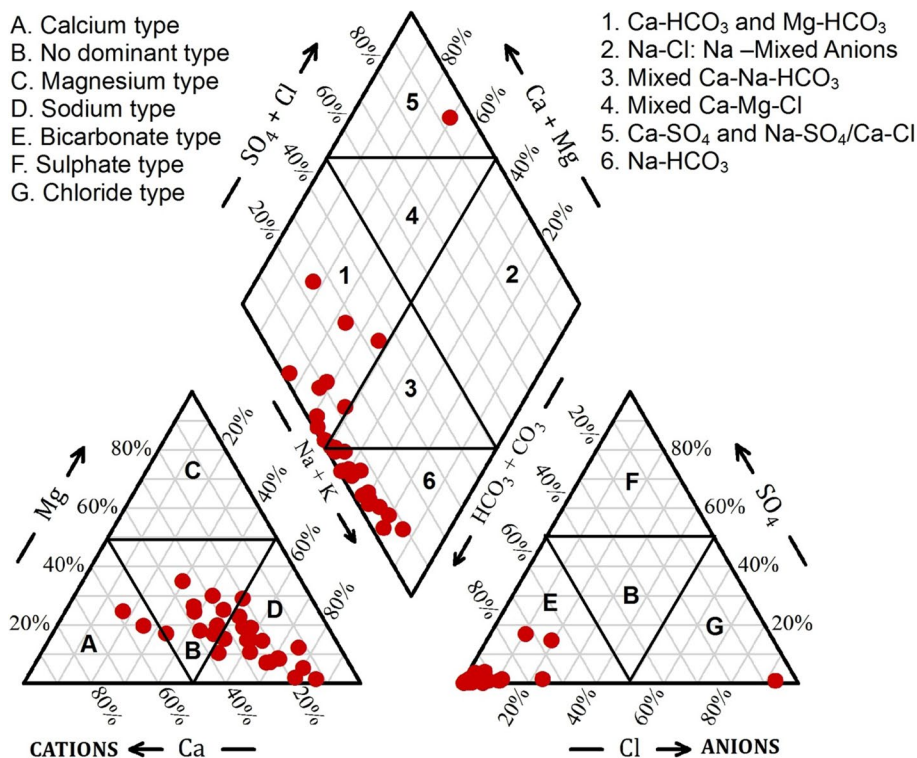
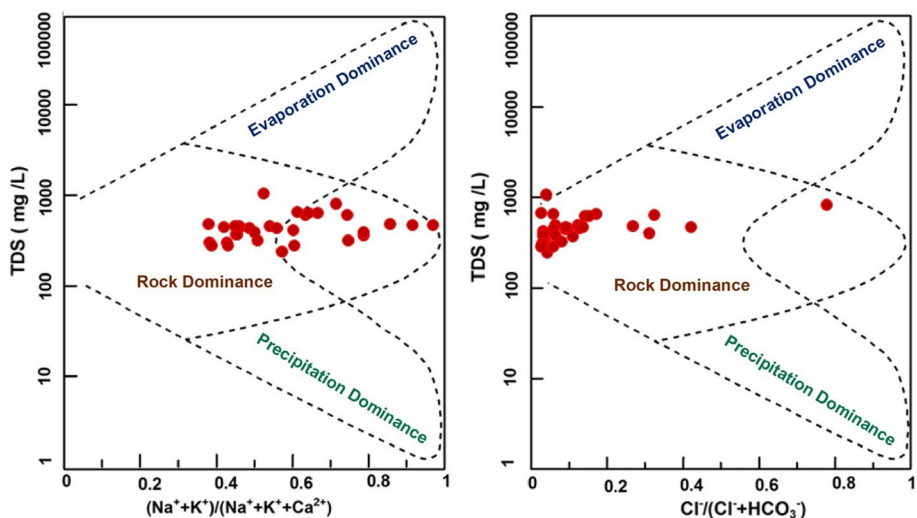


Fig. 4 Gibbs plot illustrating the hydrogeochemical processes in the basin



interaction mechanism plays a significant role in controlling groundwater chemistry in the research area. Major hydrochemical processes may be associated with rock-water interactions, ion exchange, dissolution, deposition, and redox processes (Singh et al. 2020). These interactions play an essential role in the movement and dynamics of the fluoride concentration in groundwater (Sajil Kumar 2020).

Fluoride Pollution Index and Their Spatial Distributions

The F^- concentration of groundwater in the basin varied between 0.2 and 5.6 mg/L, with an average of 2.1 mg/L (Table 4). According to the WHO drinking water quality guideline of > 1.5 mg/L, approximately 59% of the groundwater samples surpassed the limit for drinking water, and

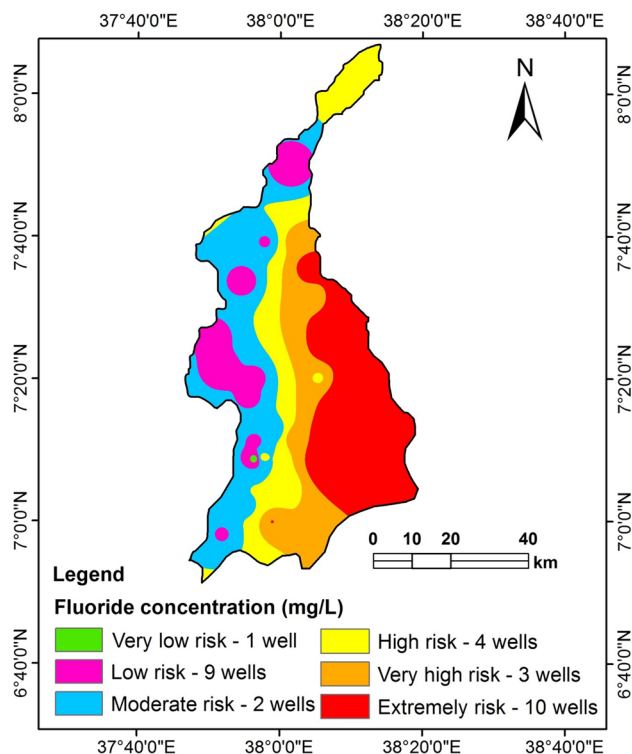


Fig. 5 Spatial variation map of groundwater fluoride risk zones

the remaining 41% of samples were acceptable for drinking but showed cause for concern over the levels of fluoride. As shown in Table 6 and Fig. 5, groundwater was divided into six categories based on the health risks from fluoride in groundwater (Aravinthasamy et al. 2019; Karunanidhi et al. 2020). In the basin, 3.5% (1 well), 31.0% (9 wells), and 6.9% (2 wells) of the samples were classified in the very low, low, and moderate risk categories, respectively. These samples were all collected in the escarpment and highlands regions in the western part of the basin. Conversely, 13.8% (4 wells) were classified under the high-risk category, while 10.3% (3 wells) and 34.5% (10 wells) of the samples were classified under the very high and extremely high-risk categories. As shown in Fig. 5 and Table 6, these samples were from groundwater in the central, southern, and southeast parts of the basin on the rift floor. The populations in these localities are highly affected by skeletal and dental fluorosis due to high fluoride concentrations in the rift valley waters (Demelash et al. 2019).

The FPI of the groundwater indicates the three major types as low, medium, and high fluoride contamination levels. The FPI values computed for each groundwater sample are shown in Table 5. In the study area, the FPI ranged from 1 to 3.5 (mean 2.6). These data clearly indicate that 51.7% of the well locations had high levels of fluoride contamination. The remaining 27.6% and 20.7%

Table 5 Computed Groundwater Quality Index (GWQI) and Fluoride Pollution Index (FPI) results

Sample no.	GWQI value	GWQI rank	Water type	FPI value	Class
1	19	1	Excellent	1	Low
2	29	1	Excellent	1.5	Low
3	26	1	Excellent	1.5	Low
4	69	2	Good	2.75	Medium
5	11	1	Excellent	1.75	Low
6	47	1	Excellent	2.25	Medium
7	23	1	Excellent	1.25	Low
8	29	1	Excellent	1.5	Low
9	113	3	Poor	2.5	Medium
10	90	2	Good	2.75	Medium
11	149	3	Poor	2.75	Medium
12	163	3	Poor	3.5	High
13	38	1	Excellent	1.75	Low
14	96	2	Good	3	High
15	120	3	Poor	3.25	High
16	131	3	Poor	3	High
17	46	1	Excellent	1.75	Low
18	82	2	Good	3	High
19	53	2	Good	3	High
20	129	3	Poor	3.25	High
21	161	3	Poor	3.25	High
22	242	4	Very poor	3.5	High
23	255	4	Very poor	3.5	High
24	103	3	Poor	3.25	High
25	150	3	Poor	3.25	High
26	54	2	Good	2.5	Medium
27	223	4	Very poor	3.5	High
28	268	4	Very poor	3.5	High
29	295	4	Very poor	3.5	High

of samples were categorized as having low and medium pollution, respectively (Table 6). Figure 6 shows that the southeastern part of the study area of 1227.6 km² is highly polluted due to the excess concentration of fluoride in groundwater. The remaining areas of 660.3 km² and 2095.5 km² are subject to low and medium water pollution, respectively. The results indicate that the groundwater in the basin is contaminated with fluoride. It indicates that rock geochemistry, such as decomposition or weathering of rocks, dissociation, and consequent dissolution, along with long residence time and high interaction of rock-water, is responsible for fluoride leaching in the basin (Shankar and Kawo 2019; Shukla and Saxena 2020a). On the other hand, the higher F⁻ in the groundwater wells can be associated to the upper pumice and to the tuff aquifers that leach the F⁻ into the subsurface water.

Table 6 Groundwater classifications and ranges of Groundwater Quality Index, the Fluoride Risk Index, the Fluoride Pollution Index, and the Total Hazard Index results

Groundwater Quality Index (GWQI)			
GWQI Ranges	Class	No. of wells	% of Wells
< 50	Excellent	9	31.03
50.01–100	Good	6	20.69
100.01–200	Poor	9	31.03
200.01–300	Very poor	5	17.24
> 300.01	Unsuitable	0	0
Fluoride Risk Index (FRI)			
F ⁻ Ranges	Risk class	No. of wells	% of wells
0.49	Very low	1	3.45
0.50–0.99	Low	9	31.03
1.00–1.49	Moderate	2	6.9
1.5–1.99	High	4	13.79
2.00–2.49	Very high	3	10.34
> 2.49	Extremely high	10	34.48
Fluoride Pollution Index (FPI)			
FPI Ranges	Class	No. of wells	% of Wells
1–2	Low	8	27.59
2–3	Medium	5	20.69
3–4	High	15	51.72
Total Hazard Index (THI)			
Humans	Health risk	No. of wells	% of wells
Male	Safe (< 1)	14	48
	Risk (> 1)	15	52
Female	Safe (< 1)	11	38
	Risk (> 1)	18	62
Children	Safe (< 1)	5	17
	Risk (> 1)	24	83

Groundwater Quality Index

The GWQI is a technique that summarizes multiple parameters of water quality in a single value to identify the suitability of water in the area for drinking water consumption. These values can be used to communicate water quality information to the community. The water quality index determines the overall quality of the groundwater at a certain site over a certain period. The GWQI values calculated for each groundwater sample are shown in Table 5. The five different water quality classes were summarized in Table 2. The minimum and maximum GWQI values in the basin were 11 and 295, respectively. GWQI values indicate that 31.0% of the samples (9 wells) had excellent quality, 20.7% of the samples (6 wells) had good quality, 31.0% of the samples (9 wells) had poor quality, and 17.2% of the samples (5 wells) had very poor quality for drinking water purposes. This

means that in the study area, 48.3% (14 wells) of the samples had poor or very poor quality for drinking purposes, and the remaining 51.7% (15 wells) have water that can be safely ingested without health risks. The spatial variation map displays that the highly affected 14 wells are distributed in the central, southern, and eastern parts of the basin and are contaminated due to geogenic sources (Fig. 7). Thus, wells distributed across approximately 1729.3 km² and 253.1 km² of the study area have poor and very poor groundwater quality. The groundwater quality is poor and very poor in the downstream part of the southern part of the basin along the escarpment to the rift floor.

Health Risk Assessment (HRA)

The HQ values calculated for children, and adult females and males showing the risks for exposure by intake of drinking

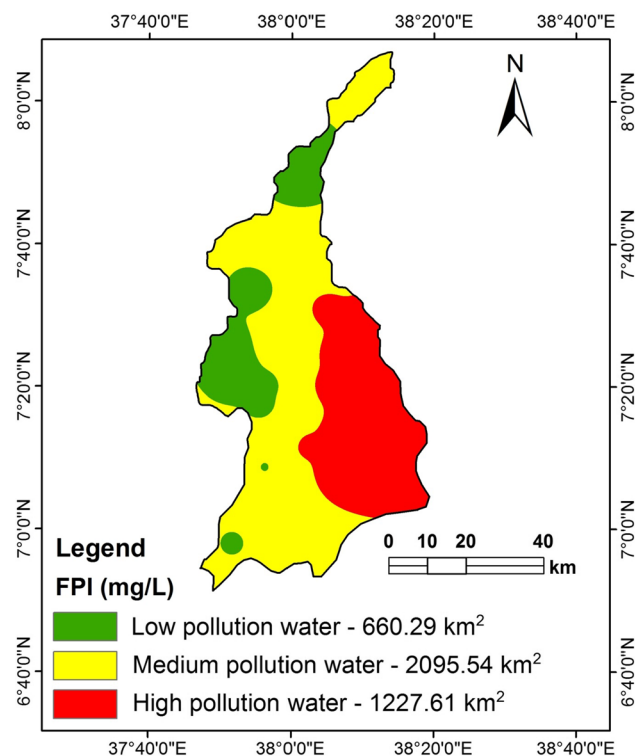


Fig. 6 Spatial variation map of FPI in the basin

water and dermal contact are summarized in Table 7. The HQ_{oral} values ranged from 0.75 to 8.40, 0.34–3.82 and 0.27–300 for children, adult females, and adult males, respectively. The HQ_{dermal} values varied from $4.00E-03$ to $4.48E-02$, $1.51E-03$ to $1.69E-02$ and $1.19E-03$ to $1.33E-02$ for children, adult females, and adult males, respectively. The THI values are in the range from 0.75 to 8.44, 0.34–3.84 and 0.27–3.01 for children, women, and men, respectively. The results show that 83%, 62% and 52% of the samples exceed the $THI > 1$ for children, females, and males as shown in Table 6 and Fig. 8. Based on the THI results, children are at higher risk compared to women and men due to their physical condition and ingestion rates. Comparative investigations have been found in various regions of the world, such as south India (Adimalla and Qian 2019; Karunanidhi et al. 2019, 2020), China (Li et al. 2016; Ji et al. 2020), and Iran (Mehdi et al. 2020). These health index data indicate that children and adult women are at greater risk than men because of the lower body weights relative to men. The body weight of individuals persons is an important determinant of health effects, as a higher body weight decreases the overall dose on a mg/kg basis. An elevated concentration of fluoride in groundwater creates health problems, such as dental and skeletal fluorosis for infants (Balamurugan et al. 2020b). Continuous intake of fluoride contaminated water tends to cause fluorosis, bone and teeth disease, and spinal disorders.

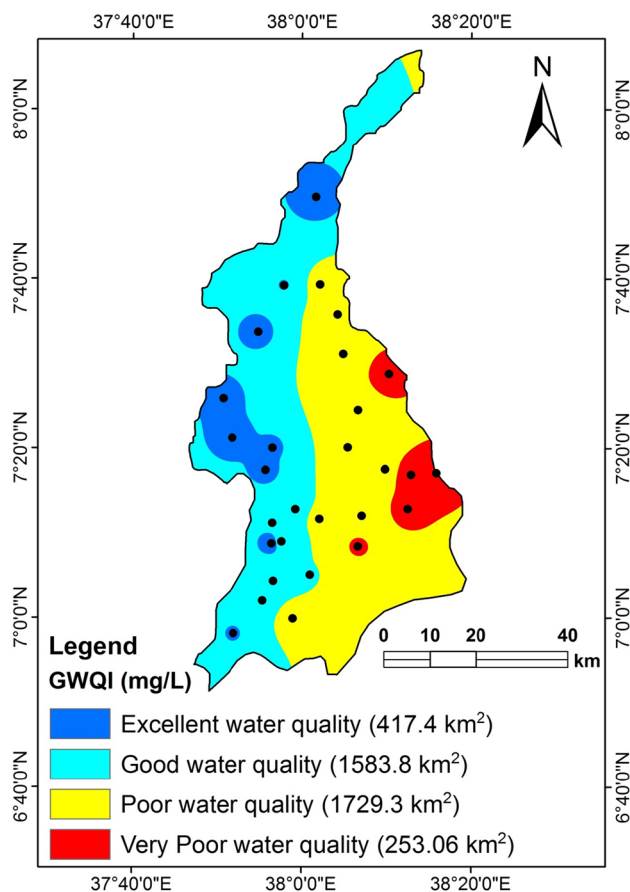


Fig. 7 Spatial variation map of GWQI in the Bilate River basin

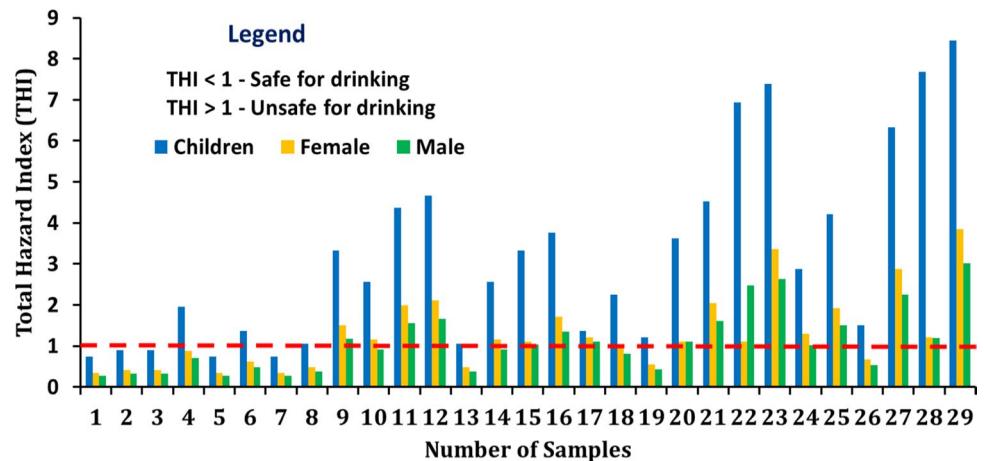
Conclusions

For the present research investigation, 29 groundwater samples were collected from the Bilate River Basin of the southern Main Ethiopian Rift and were analyzed with physicochemical parameters to assess the suitability of groundwater using GWQI, FPI, and GIS tools and to assess the risk factors for human health associated with fluoride in groundwater. The major outcomes of the research indicate that the groundwater in the basin shows a systematic hydrochemical evolution from the slightly mineralized and relatively young highland Ca–Mg–HCO₃ water type to the moderately mineralized Na–Ca–HCO₃ water type in the rift escarpment and finally to the highly mineralized Na–HCO₃ water type on the rift floor, following the groundwater flow path from the highlands to the rift floor. According to the GWQI, 48.3% of the groundwater samples were categorized within the poor and very poor water quality categories, while the remaining wells contain groundwater that can be safely ingested without any health risks. The F⁻ concentrations measured in groundwater indicated that 58.6% (17 wells) of the samples surpassed the limit for drinking water of 1.5 mg/L. According to the FPI, 51.7% of the wells were found to be

Table 7 Assessment results for health risks through oral consumption of drinking water and through dermal contact calculated for children and adult males and females

Sample no.	HQ _{oral}			HQ _{dermal}			THI		
	Children	Female	Male	Children	Female	Male	Children	Female	Male
1	0.75	0.34	0.27	4.00E-03	1.51E-03	1.19E-03	0.75	0.34	0.27
2	0.90	0.41	0.32	4.80E-03	1.81E-03	1.42E-03	0.90	0.41	0.32
3	0.90	0.41	0.32	4.80E-03	1.81E-03	1.42E-03	0.90	0.41	0.32
4	1.95	0.89	0.70	1.04E-02	3.92E-03	3.08E-03	1.96	0.89	0.70
5	0.75	0.34	0.27	4.00E-03	1.51E-03	1.19E-03	0.75	0.34	0.27
6	1.35	0.61	0.48	7.20E-03	2.72E-03	2.13E-03	1.36	0.62	0.48
7	0.75	0.34	0.27	4.00E-03	1.51E-03	1.19E-03	0.75	0.34	0.27
8	1.05	0.48	0.38	5.60E-03	2.11E-03	1.66E-03	1.06	0.48	0.38
9	3.30	1.50	1.18	1.76E-02	6.64E-03	5.22E-03	3.32	1.51	1.18
10	2.55	1.16	0.91	1.36E-02	5.13E-03	4.03E-03	2.56	1.16	0.91
11	4.35	1.98	1.55	2.32E-02	8.75E-03	6.88E-03	4.37	1.99	1.56
12	4.65	2.11	1.66	2.48E-02	9.36E-03	7.35E-03	4.67	2.12	1.67
13	1.05	0.48	0.38	5.60E-03	2.11E-03	1.66E-03	1.06	0.48	0.38
14	2.55	1.16	0.91	1.36E-02	5.13E-03	4.03E-03	2.56	1.16	0.91
15	3.30	1.10	1.02	1.76E-02	6.64E-03	5.22E-03	3.32	1.11	1.03
16	3.75	1.70	1.34	2.00E-02	7.55E-03	5.93E-03	3.77	1.71	1.35
17	1.35	1.21	1.10	7.20E-03	2.72E-03	2.13E-03	1.36	1.21	1.10
18	2.25	1.02	0.80	1.20E-02	4.53E-03	3.56E-03	2.26	1.03	0.81
19	1.20	0.55	0.43	6.40E-03	2.41E-03	1.90E-03	1.21	0.55	0.43
20	3.60	1.09	1.09	1.92E-02	7.24E-03	5.69E-03	3.62	1.10	1.10
21	4.50	2.05	1.61	2.40E-02	9.05E-03	7.11E-03	4.52	2.05	1.61
22	6.90	1.10	2.46	3.68E-02	1.39E-02	1.09E-02	6.94	1.11	2.48
23	7.35	3.34	2.63	3.92E-02	1.48E-02	1.16E-02	7.39	3.36	2.64
24	2.85	1.30	1.02	1.52E-02	5.73E-03	4.51E-03	2.87	1.30	1.02
25	4.20	1.91	1.50	2.24E-02	8.45E-03	6.64E-03	4.22	1.92	1.51
26	1.50	0.68	0.54	8.00E-03	3.02E-03	2.37E-03	1.51	0.68	0.54
27	6.30	2.86	2.25	3.36E-02	1.27E-02	9.96E-03	6.33	2.88	2.26
28	7.65	1.20	1.19	4.08E-02	1.54E-02	1.21E-02	7.69	1.22	1.20
29	8.40	3.82	3.00	4.48E-02	1.69E-02	1.33E-02	8.44	3.84	3.01
Minimum	0.75	0.34	0.27	4.00E-03	1.51E-03	1.19E-03	0.75	0.34	0.27
Maximum	8.40	3.82	3.00	4.48E-02	1.69E-02	1.33E-02	8.44	3.84	3.01

Fig. 8 Calculated Total hazard index (THI) for all the ground-water samples collected from the basin to assess the health risks for children, males, and females



highly polluted due to the excess concentrations of fluoride in groundwater. The THI showed that 83%, 62% and 52% of the samples exceeded the noncarcinogenic health risk for consumption of fluoride in drinking water for children, female adults, and male adults, respectively. Based on the THI results, children are at the greatest risk for health effects from ingestion of contaminated groundwater.

Overall, the data generated from this study shows an alarming level of health risks from fluoride contamination of groundwater among the population inhabiting the Bilate River Basin of the Southern Main Ethiopian Rift. Ethiopia is challenged by a struggling economy and conflicts in some areas of the country, but attention is needed on the part of the Ethiopian government and international health agencies to alleviate the health risks associated with fluoride contamination of the sources of drinking water.

Acknowledgments The authors thank the Editor-in-Chief and anonymous reviewers for their meticulous assessment and significant comments that helped to strengthen the manuscript quality.

Compliance with Ethical Standards

Conflict of interest The authors declare that they have no conflict of interest.

References

- Abbate E, Bruni P, Sagri M (2015) Geology of Ethiopia: a review and geomorphological perspectives. In: Billi P (ed) *Landscapes and landforms of Ethiopia*. Springer, Dordrecht, pp 33–64. <https://doi.org/10.1007/978-94-017-8026-1>
- Adimalla N (2019) Controlling factors and mechanism of groundwater quality variation in semiarid region of South India: an approach of water quality index (WQI) and health risk assessment (HRA). *Environ Geochem Health* 42:1725–1752. <https://doi.org/10.1007/s10653-019-00374-8>
- Adimalla N, Li P (2019) Occurrence, health risks, and geochemical mechanisms of fluoride and nitrate in groundwater of the rock dominant semi-arid region, Telangana State, India. *Hum Ecol Risk Assess* 25(1–2):81–103. <https://doi.org/10.1080/10807039.2018.1480353>
- Adimalla N, Qian H (2019) Groundwater quality evaluation using water quality index (WQI) for drinking purposes and human health risk (HHR) assessment in an agricultural region of Nanganur, south India. *Ecotoxicol Environ Saf* 176:153–161. <https://doi.org/10.1016/j.ecoenv.2019.03.066>
- Adimalla N, Wu J (2019) Groundwater quality and associated health risks in a semi-arid region of South India: implication to sustainable groundwater management. *Hum Ecol Risk Assess* 25(1–2):191–216. <https://doi.org/10.1080/10807039.2018.1546550>
- Alemayehu T (2006) *Groundwater occurrence in Ethiopia*. UNESCO, Paris
- Amanuel G (2018) Geospatial distribution modeling and determining suitability of groundwater quality for irrigation purpose using geospatial methods and water quality index (WQI) in Northern Ethiopia. *Appl Water Sci* 8(3):1–16. <https://doi.org/10.1007/s13201-018-0722-x>
- APHA (2012) *Standard methods for the examination of water and wastewater*, 22nd edn. American Public Health Association, Washington, DC
- Aravindan S, Shankar K (2011) Ground water quality maps of Paravandar river sub basin, Cuddalore District, Tamil Nadu, India. *J Indian Soc Remote Sens* 39(4):565–581. <https://doi.org/10.1007/s12524-011-0152-9>
- Aravindan S, Shankar K, Mini SS (2011) Integrated geohydrological studies in the sedimentary part of Gadilam River Basin, Cuddalore District, Tamil Nadu. *Asian J Earth Sci* 4:183–192. <https://doi.org/10.3923/ajes.2011.183.192>
- Aravinthasamy P, Karunanidhi D, Subramani T, Srinivasamoorthy K, Anand B (2019) Geochemical evaluation of fluoride contamination in groundwater from Shanmuganadhi River basin, South India: implication on human health. *Environ Geochem Health*. <https://doi.org/10.1007/s10653-019-00452-x>
- Arya S, Subramani T, Vennila G, Karunanidhi D (2019) Health risks associated with fluoride intake from rural drinking water supply and inverse mass balance modeling to decipher hydro-geochemical processes in Vattamalaikarai River basin South India. *Environ Geochem Health*. <https://doi.org/10.1007/s10653-019-00489-y>
- Athick AMA, Shankar K (2019) Data on land use and land cover changes in Adama Wereda, Ethiopia, on ETM⁺, TM and OLI-TIRS Landsat sensor using PCC and CDM techniques. *Data Brief*. <https://doi.org/10.1016/j.dib.2019.103880>
- Ayene T (2008) The distribution and hydrogeological controls of fluoride in the groundwater of Central Ethiopian Rift and adjacent highlands. *Environ Geol* 54:1313–1324. <https://doi.org/10.1007/s00254-007-0914-4>
- Balamurugan P, Kumar PS, Shankar K (2020a) Dataset on the suitability of groundwater for drinking and irrigation purposes in the Sarabanga River region, Tamil Nadu, India. *Data Brief* 29:105255. <https://doi.org/10.1016/j.dib.2020.105255>
- Balamurugan P, Kumar PS, Shankar K, Nagavinoothini R, Vijayasurya K (2020b) Non-carcinogenic risk assessment of groundwater in southern part of Salem District in Tamilnadu, India. *J Chilean Chem Soc* 65(1):4697–4707. <https://doi.org/10.4067/S0717-97072020000104697>
- Chandrajith R, Padmasiri JP, Dissanayake CB, Prematilaka KM (2012) Spatial distribution of fluoride in groundwater of Sri Lanka. *J Natl Sci Found Sri Lanka* 40(4):303–309. <https://doi.org/10.4038/jnsfr.v40i4.5044>
- Corti G, Sani F, Philippon M, Sokoutis D, Willingshofer E, Molin P (2013) Quaternary volcano-tectonic activity in the Soddò region, western margin of the Southern Main Ethiopian Rift. *Tectonics* 32(4):861–879. <https://doi.org/10.1002/tect.20052>
- Deepa S, Venkateswaran S (2018) Appraisal of groundwater quality in upper Manimuktha sub basin, Vellar river, Tamil Nadu, India by using water quality index (WQI) and multivariate statistical techniques. *Model Earth Syst Environ* 4(3):1165–1180. <https://doi.org/10.1007/s40808-018-0468-3>
- Demelash H, Beyene A, Abebe Z, Melese A (2019) Fluoride concentration in ground water and prevalence of dental fluorosis in Ethiopian Rift Valley: systematic review and meta-analysis. *BMC Publ Health* 19(1):1298. <https://doi.org/10.1186/s12889-019-7646-8>
- Demlie M, Wöhllich S (2006) Soil and groundwater pollution of an urban catchment by trace metals: case study of the Addis Ababa region, central Ethiopia. *J Environ Geol* 51(3):421–431. <https://doi.org/10.1007/s00254-006-0337-7>
- Di Paola GM (1972) The Ethiopian rift valley (between 7°00' and 8°40' lat. North). *Bull Volc* 36(4):517–560
- Furi W, Razack M, Haile T, Abiye TA, Legesse D (2010) The hydrogeology of Adama–Wonji basin and assessment of groundwater level changes in Wonji wetland, Main Ethiopian Rift: results from 2D tomography and electrical sounding methods. *Environ*

- Earth Sci 62(6):1323–1335. <https://doi.org/10.1007/s12665-010-0619-y>
- Furi W, Razack Moutmaz, Abiye TamiruAlemayehu, Legesse TenalemAyenewDagnachew (2011) Fluoride enrichment mechanism and geospatial distribution in the volcanic aquifers of the Middle Awash basin, Northern Main Ethiopian Rift. *J Afr Earth Sci* 60:315–327. <https://doi.org/10.1016/j.jafrearsci.2011.03.004>
- Furi W, Razack M, Abiye TA, Kebede S, Legesse D (2012) Hydrochemical characterization of complex volcanic aquifers in a continental rifted zone: the Middle Awash basin, Ethiopia. *Hydrogeol J* 20:385. <https://doi.org/10.1007/s10040-011-0807-1>
- Gaikwad SK, Kadam AR, Ramgir RR, Kashikar AS, Wagh VM, Kandekar AM, Kamble KD et al (2020) Assessment of the groundwater geochemistry from a part of west coast of India using statistical methods and water quality index. *Hydrol Res* 3:48–60. <https://doi.org/10.1016/j.hydres.2020.04.001>
- Gebere A, Kawo NS, Karuppanan S et al (2020) Numerical modeling of groundwater flow system in the Modjo River catchment, Central Ethiopia. *Model Earth Syst Environ*. <https://doi.org/10.1007/s40808-020-01040-0>
- Getnet TB, Zelalem LA (2020) Spatial assessment and appraisal of groundwater suitability for drinking consumption in Andasa watershed using water quality index (WQI) and GIS techniques: Blue Nile Basin, Northwestern Ethiopia. *Cogent Eng* 7(1):1748950. <https://doi.org/10.1080/23311916.2020.1748950>
- Gibbs RJ (1970) Mechanisms controlling world water chemistry. *Science* 17:1088–1090. <https://doi.org/10.1126/science.170.3962.1088>
- Haile T, Abiye TA (2012) The interference of a deep thermal system with a shallow aquifer: the case of Sodere and Gergedi thermal springs, Main Ethiopian Rift, Ethiopia. *Hydrogeol J* 20(3):561–574. <https://doi.org/10.1007/s10040-012-0832-8>
- Haji M, Wang D, Li L, Qin D, Guo Y (2018) Geochemical evolution of fluoride and implication for F⁻ enrichment in groundwater: example from the Bilate River Basin of Southern Main Ethiopian Rift. *Water* 10(12):1799. <https://doi.org/10.3390/w10121799>
- He X, Li P (2020) Surface water pollution in the middle Chinese Loess Plateau with special focus on hexavalent chromium (Cr⁶⁺): occurrence, sources and health risks. *Expo Health* 12(3):385–401. <https://doi.org/10.1007/s12403-020-00344-x>
- He S, Wu J (2019) Relationships of groundwater quality and associated health risks with land use/land cover patterns: a case study in a loess area, northwest China. *Hum Ecol Risk Assess* 25(1–2):354–373. <https://doi.org/10.1080/10807039.2019.1570463>
- He S, Li P, Wu J, Elumalai V, Adimalla N (2019) Groundwater quality under land use/land cover changes: a temporal study from 2005 to 2015 in Xi'an, Northwest China. *Hum Ecol Risk Assess*. <https://doi.org/10.1080/10807039.2019.1684186>
- He X, Li P, Ji Y, Wang Y, Su Z, Elumalai V (2020a) Groundwater arsenic and fluoride and associated arsenicosis and fluorosis in China: occurrence, distribution and management. *Expo Health* 12(3):355–368. <https://doi.org/10.1007/s12403-020-00347-8>
- He X, Li P, Wu J, Wei M, Ren X, Wang D (2020b) Poor groundwater quality and high potential health risks in the Datong Basin, northern China: research from published data. *Environ Geochem Health*. <https://doi.org/10.1007/s10653-020-00520-7>
- Hounslow AW (1995) Water quality data analysis and interpretation. CRC Press, Boca Raton
- Hussen B, Wagesho N (2016) Regional flood frequency analysis for Abaya–Chamo sub basin, rift valley basin, Ethiopia. *J Resour Dev Manag* 24:15–28
- Hutchison W, Pyle DM, Mather TA, Yirgu G, Biggs J, Cohen BE et al (2016) The eruptive history and magmatic evolution of Aluto volcano: new insights into silicic peralkaline volcanism in the Ethiopian rift. *J Volcanol Geotherm Res* 328:9–33. <https://doi.org/10.1016/j.jvolgeores.2016.09.010>
- IAEA (2013) Assessing and managing groundwater in Ethiopia. International Atomic Energy Agency, Vienna
- Ji Y, Wu J, Wang Y, Elumalai V, Subramani T (2020) Seasonal variation of drinking water quality and human health risk assessment in Hancheng City of Guanzhong Plain, China. *Expo Health* 12(3):469–485. <https://doi.org/10.1007/s12403-020-00357-6>
- Kadam A, Vasant Wagh, Umrikar B, Sankhua R (2019) An implication of boron and fluoride contamination and its exposure risk in groundwater resources in semi-arid region. *Environ Dev Sustain Western India*. <https://doi.org/10.1007/s10668-019-00527-w>
- Kalaivanan K, Gurugnanam B, Pourghasemi HR, Suresh M, Kumaravel S (2017) Spatial assessment of groundwater quality using water quality index and hydrochemical indices in the Kodavaran sub-basin, Tamil Nadu, India. *Sustain Water Resour Manag* 4(3):627–641. <https://doi.org/10.1007/s40899-017-0148-x>
- Karunanidhi D, Aravinthasamy P, Subramani T, Wu J, Srinivasamoorthy K (2019) Potential health risk assessment for fluoride and nitrate contamination in hard rock aquifers of Shanmuganadhi River basin, South India. *Hum Ecol Risk Assess* 25(1–2):250–270. <https://doi.org/10.1080/10807039.2019.1568859>
- Karunanidhi D, Aravinthasamy P, Subramani T, Balakumar KG, Chandran NS (2020) Health threats for the inhabitants of a textile hub (Tiruppur region) in southern India due to multipath entry of fluoride ions from groundwater. *Ecotoxicol Environ Saf* 204:111071. <https://doi.org/10.1016/j.ecoenv.2020.111071>
- Kavitha MT, Divahar R, Meenambal T, Shankar K, VijaySingh R, Haile TamiratDessalegn, Gadafa Chimdi (2019a) Dataset on the assessment of water quality of surface water in Kalingarayan Canal for heavy metal pollution, Tamil Nadu. *Data Brief* 22:878–884. <https://doi.org/10.1016/j.dib.2019.01.010>
- Kavitha MT, Shankar K, Divahar R, Meenambal T, Saravanan R (2019b) Impact of industrial wastewater disposal on surface water bodies in Kalingarayan canal, Erode district, Tamil Nadu, India. *Arch Agric Environ Sci* 4(4):379–387. <https://doi.org/10.26832/24566632.2019.040403>
- Kawo NS, Shankar K (2018) Groundwater quality assessment using water quality index and GIS technique in Modjo River Basin, Central Ethiopia. *J Afr Earth Sci* 147:300–311. <https://doi.org/10.1016/j.jafrearsci.2018.06.034>
- Kebede S (2013) Groundwater in Ethiopia, features, numbers and opportunities. Springer, Berlin
- Kebede S, Travi Y, Stadler S (2010) Groundwaters of the Central Ethiopian Rift: diagnostic trends in trace elements, d¹⁸O and major elements. *Environ Earth Sci* 61:1641–1655
- Kebede S, Hailu A, Crane E, Dochartaigh B (2016) Africa groundwater atlas: hydrogeology of Ethiopia. British Geological Survey, Nottingham, pp 1–17
- Li P (2016) Groundwater quality in western China: challenges and paths forward for groundwater quality research in western China. *Expo Health* 8(3):305–310. <https://doi.org/10.1007/s12403-016-0210-1>
- Li P, Li X, Meng X, Li M, Zhang Y (2016) Appraising groundwater quality and health risks from contamination in a semiarid region of northwest China. *Expo Health* 8(3):361–379. <https://doi.org/10.1007/s12403-016-0205-y>
- Li P, Tian R, Xue C, Wu J (2017) Progress, opportunities and key fields for groundwater quality research under the impacts of human activities in China with a special focus on western China. *Environ Sci Pollut Res* 24(15):13224–13234. <https://doi.org/10.1007/s11356-017-8753-7>
- Li P, He S, Yang N, Xiang G (2018) Groundwater quality assessment for domestic and agricultural purposes in Yan'an City, northwest China: implications to sustainable groundwater quality management on the Loess Plateau. *Environ Earth Sci* 77(23):775. <https://doi.org/10.1007/s12665-018-7968-3>

- Li P, He X, Li Y, Xiang G (2019) Occurrence and health implication of fluoride in groundwater of Loess aquifer in the Chinese Loess Plateau: a case study of Tongchuan, northwest China. *Expo Health* 11(2):95–107. <https://doi.org/10.1007/s12403-018-0278-x>
- Mechal A, Birk S, Dietzel M, Leis A, Winkler G, Mogessie A, Kebede S (2017) Groundwater flow dynamics in the complex aquifer system of Gidabo River Basin (Ethiopian Rift): a multi-proxy approach. *Hydrogeol J* 25:519–538. <https://doi.org/10.1007/s10040-016-1489-5>
- Mehdi Q, Mansoureh F, Maryam M, Maryam M, Sara E, Ali A, Javad B, Ahmad Z, Javad B, Mojtaba A, Sahar G, Afshin G (2020) Investigation of potential human health risks from fluoride and nitrate via water consumption in Sabzevar. *Iran. Int J Environ Anal Chem.* <https://doi.org/10.1080/03067319.2020.1720668>
- Mousazadeh H, Mahmudy-Gharaie MH, Mosaedi A, Moussavi Harami R (2018) Hydrochemical assessment of surface and ground waters used for drinking and irrigation in Kardeh Dam Basin (NE Iran). *Environ Geochem Health.* <https://doi.org/10.1007/s10653-018-0214-9>
- Mukate S, Wagh V, Panaskar D, Jacobs JA, Sawant A (2019) Development of new integrated water quality index (IWQI) model to evaluate the drinking suitability of water. *Ecol Indic* 101:348–354. <https://doi.org/10.1016/j.ecolind.2019.01.034>
- Panneerselvam B, Paramasivam SK, Karuppannan S et al (2020a) A GIS-based evaluation of hydrochemical characterisation of groundwater in hard rock region, South Tamil Nadu, India. *Arab J Geosci* 13(17):1–22. <https://doi.org/10.1007/s12517-020-05813-w>
- Panneerselvam B, Karuppannan S, Muniraj K (2020b) Evaluation of drinking and irrigation suitability of groundwater with special emphasizing the health risk posed by nitrate contamination using nitrate pollution index (NPI) and human health risk assessment (HHRA). *Hum Ecol Risk Assess Int J.* <https://doi.org/10.1080/10807039.2020.1833300>
- Peng C, He JT, Wang M, Zhang Z, Wang L (2018) Identifying and assessing human activity impacts on groundwater quality through hydrogeochemical anomalies and NO_3^- , NH_4^+ , and COD contamination: a case study of the Liujiang River Basin, Hebei Province, PR China. *Environ Sci Pollut Res* 25(4):3539–3556. <https://doi.org/10.1007/s11356-017-0497-x>
- Piper AM (1944) A graphic procedure in the chemical interpretation of water analysis. *Am Geophys Union Trans* 25:914–923
- Prasad NBN (1984) Hydrogeological studies in the Bhadra River Basin. Ph.D. Thesis, University of Mysore, Karnataka, India, p 323
- Qin R, Wu Y, Xu Z, Xie D, Zhang C (2013) Assessing the impact of natural and anthropogenic activities on groundwater quality in coastal alluvial aquifers of the lower Liaohe River Plain, NE China. *Appl Geochem* 31:142–158. <https://doi.org/10.1016/j.apgeochem.2013.01.001>
- Rafique T, Naseem S, Bhangar MI, Usmani TH (2008) Fluoride ion contamination in the groundwater of Mithi sub-district, the Thar Desert, Pakistan. *Environ Geol* 56:317–326. <https://doi.org/10.1007/s00254-007-1167-y>
- Rango T, Bianchini G, Beccaluva L, Ayenew T, Colombani N (2009) Hydrogeochemical study in the Main Ethiopian Rift: new insights to the source and enrichment mechanism of fluoride. *Environ Geol* 58:109–118. <https://doi.org/10.1007/s00254-008-1498-3>
- Rango T, Bianchini G, Beccaluva L, Tassinari R (2010) Geochemistry and water quality assessment of central Main Ethiopian Rift natural waters with emphasis on source and occurrence of fluoride and arsenic. *J Afr Earth Sci* 57(5):479–491. <https://doi.org/10.1016/j.jafrearsci.2009.12.005>
- Rango T, Kravchenko J, Atlaw B, McCornick PeterG, Jeuland M, Merola B, Vengosh A (2012) Groundwater quality and its health impact, an assessment of dental fluorosis in rural inhabitants of the Main Ethiopian Rift. *Environ Int* 43:37–47. <https://doi.org/10.1016/j.envint.2012.03.002>
- Rufino F, Busico G, Cuoco E, Darrah TH, Tedesco D (2019) Evaluating the suitability of urban groundwater resources for drinking water and irrigation purposes: an integrated approach in the Agro-Aversano area of Southern Italy. *Environ Monit Assess* 191(12):768. <https://doi.org/10.1007/s10661-019-7978-y>
- Sahu P, Sikdar PK (2008) Hydrochemical framework of the aquifer in and around East Kolkata wetlands, West Bengal, India. *Environ Geol* 55:823–835. <https://doi.org/10.1007/s00254-007-1034-x>
- Sajil Kumar PJ (2017) A proposed method for the quantification of fluoride contamination: fluoride pollution index (FPI). *Geochem J* 4:1–4
- Sajil Kumar PJ (2020) Fluoride enrichment in groundwater and associated human health risk in a tropical hard rock terrain in South India. *Hum Ecol Risk Assess Int J.* <https://doi.org/10.1080/10807039.2020.1799185>
- Saleem M, Hussain A, Mahmood G (2016) Analysis of groundwater quality using water quality index: a case study of greater Noida (Region), Uttar Pradesh (UP), India. *Cogent Eng* 3(1):1237927. <https://doi.org/10.1080/23311916.2016.1237927>
- Shankar K, Kawo NS (2019) Groundwater quality assessment using geospatial techniques and WQI in North East of Adama Town, Oromia Region, Ethiopia. *Hydrospatial Anal* 3(1):22–36. <https://doi.org/10.21523/gcj3.19030103>
- Shankar K, Aravindan S, Rajendran S (2011a) Hydrogeochemistry of the Paravanan river sub-basin, Cuddalore District, Tamilnadu, India. *E-J Chem* 8(2):835–845. <https://doi.org/10.1155/2011/107261>
- Shankar K, Aravindan S, Rajendran S (2011b) Hydrochemical profile for assessing the groundwater quality of Paravanan River Sub-Basin, Cuddalore district, Tamil Nadu, India. *Curr World Environ* 6(1):45–52. <https://doi.org/10.12944/CWE.6.1.05>
- Shankar K, Aravindan S, Rajendran S (2011c) Assessment of groundwater quality in Paravanan River Sub-Basin, Cuddalore district, Tamil Nadu, India. *Adv Appl Sci Res* 2(5):92–103
- Shukla S, Saxena A (2020a) Groundwater quality and associated human health risk assessment in parts of Raebareli district, Uttar Pradesh, India. *Groundw Sustain Dev* 10:100366. <https://doi.org/10.1016/j.gsd.2020.100366>
- Shukla S, Saxena A (2020b) Appraisal of groundwater quality with human health risk assessment in parts of Indo-Gangetic alluvial plain, North India. *Arch Environ Contam Toxicol.* <https://doi.org/10.1007/s00244-020-00771-6>
- Singh UK, Kumar B (2017) Pathways of heavy metals contamination and associated human health risk in Ajay River basin, India. *Chemosphere* 174:183–199. <https://doi.org/10.1016/j.chemosphere.2017.01.103>
- Singh A, Patel AK, Kumar M (2020) Mitigating the risk of arsenic and fluoride contamination of groundwater through a multi-model framework of statistical assessment and natural remediation techniques. In: *Emerging issues in the water environment during anthropocene*. Springer, Singapore, pp 285–300
- Soujanya Kamble B, Saxena PR, Kurakalva RM, Shankar K (2020) Evaluation of seasonal and temporal variations of groundwater quality around Jawaharnagar municipal solid waste dumpsite of Hyderabad city, India. *SN Appl Sci* 2(3):498. <https://doi.org/10.1007/s42452-020-2199-0>
- Su F, Li P, He X, Elumalai V (2020a) Set pair analysis in earth and environmental sciences: development, challenges, and future prospects. *Expo Health* 12(3):343–354. <https://doi.org/10.1007/s12403-020-00368-3>

- Su Z, Wu J, He X, Elumalai V (2020b) Temporal changes of groundwater quality within the groundwater depression cone and prediction of confined groundwater salinity using Grey Markov model in Yinchuan area of northwest China. *Expo Health* 12(3):447–468. <https://doi.org/10.1007/s12403-020-00355-8>
- Tian R, Wu J (2019) Groundwater quality appraisal by improved set pair analysis with game theory weightage and health risk estimation of contaminants for Xuecha drinking water source in a loess area in Northwest China. *Hum Ecol Risk Assess Int J* 25(1–2):132–157. <https://doi.org/10.1080/10807039.2019.1573035>
- Todd DK, Mays LW (2005) *Groundwater hydrology*. Wiley, Hoboken
- Tolera MB, Choi H, Chang SW, Chung I-M (2020) Groundwater quality evaluation for different uses in the lower Ketar Watershed, Ethiopia. *Environ Geochem Health*. <https://doi.org/10.1007/s10653-019-00508-y>
- United States Environmental Protection Agency (USEPA) (1989) *Superfund public health evaluation manual*. Washington, DC
- US Environmental Protection Agency (USEPA) (2001) *Baseline human health risk assessment Vasquez Boulevard and I-70 superfund site, Denver CO*. <http://www.epa.gov/region8/superfund/sites/VB-170-Risk.pdf>. Accessed 20 Jan 2011
- Varis O (2014) Resources: curb vast water use in central Asia. *Nat News* 514(7520):27
- Vasquez LV, Hernandez JR, Lopez JR, Uribe AS, Mancilla OL (2006) The origin of fluoride in groundwater supply to Hermosillo City, Sonora, Mexico. *Environ Geol* 51:17–27. <https://doi.org/10.1007/s00254-006-0300-7>
- Wagh VM, Panaskar DB, Shrikant VM, Manesh LA, Uday LS (2019a) Nitrate associated health risks from groundwater of Kadava River Basin Nashik, Maharashtra, India. *Hum Ecol Risk Assess Int J*. <https://doi.org/10.1080/10807039.2018.1528861>
- Wagh VM, Panaskar DB, Jacobs JA, Mukate SV, Muley AA, Kadam AK (2019b) Influence of hydro-geochemical processes on groundwater quality through geostatistical techniques in Kadava River basin, Western India. *Arab J Geosci* 12(1):7. <https://doi.org/10.1007/s12517-018-4136-8>
- Wang D, Wu J, Wang Y, Ji Y (2020) Finding high-quality groundwater resources to reduce the hydatidosis incidence in the Shiqu County of Sichuan Province, China: analysis, assessment, and management. *Expo Health* 12(2):307–322. <https://doi.org/10.1007/s12403-019-00314-y>
- WHO (2011) *World health organisation guidelines for drinking water quality, 4th edn*. In: *Incorporating the first and second addenda, 1 Recommendation* (Geneva)
- WHO (2017) *Guidelines for drinking water quality: fourth edition incorporating the first addendum, 4th edn*. World Health Organization, Geneva
- Wu J, Zhou H, He S, Zhang Y (2019) Comprehensive understanding of groundwater quality for domestic and agricultural purposes in terms of health risks in a coal mine area of the Ordos basin, north of the Chinese Loess Plateau. *Environ Earth Sci* 78(15):446. <https://doi.org/10.1007/s12665-019-8471-1>
- WWDR (2015) *Water for a sustainable world*. France: The United Nations Educational, Scientific and Cultural Organization
- Yadav KK, Kumar V, Gupta N, Kumar S, Rezaia S, Singh N (2019) Human health risk assessment: study of a population exposed to fluoride through groundwater of Agra city, India. *Regul Toxicol Pharmacol* 106:68–80. <https://doi.org/10.1016/j.yrtph.2019.04.013>
- Yitbarek A, Razack M, Ayenew T, Zemedagegnehu E, Azagegn T (2012) Hydrogeological and hydrochemical framework of Upper Awash River basin, Ethiopia: with special emphasis on inter-basins groundwater transfer between Blue Nile and Awash Rivers. *J Afr Earth Sci* 65:46–60. <https://doi.org/10.1016/j.jafrearsci.2012.01.002>